Journal of
Synchrotron
Radiation

ISSN 0909-0495

Received 21 January 2008
Accepted 7 July 2009

Novel high-temperature reactors for *in situ* studies of three-way catalysts using turbo-XAS

Gemma Guilera,[a]*‡ Bernard Gorges,[a] Sakura Pascarelli,[a] Hugo Vitoux,[a] Mark A. Newton,[a] Carmelo Prestipino,[a] Yasutaka Nagai[b] and Naoyuki Hara[c]

[a]ESRF, 6 rue Jules Horowitz, 38043 Grenoble Cedex, France, [b]Toyota Central R&D Laboratory, Nagakute, Aichi 480-1192, Japan, and [c]Toyota Motor Europe Technical Centre, B-1930 Zaventem, Belgium. E-mail: gemma.guilera@cells.es

Two novel high-temperature reactors for *in situ* X-ray absorption spectroscopy (XAS) measurements in fluorescence are presented, each of them being optimized for a particular purpose. The powerful combination of these reactors with the turbo-XAS technique used in a dispersive-XAS beamline permits the study of commercial three-way catalysts under realistic gas composition and temporal conditions.

Keywords: *in situ* reactor; turbo-XANES; time-resolved experiment; three-way catalysts.

1. Introduction

Three-way catalysts (TWCs) have been used to control gasoline-fuelled vehicle emissions for over 20 years and they are still one of the most widely used catalysts in automobile commerce. Relentless efforts are being made to improve catalyst performance, reduce costs and, most importantly, meet the increasingly stringent regulations regarding toxic gas emissions produced in spark ignition engines (CO, NO_x and unburned hydrocarbons).

Investigation of TWCs at the atomic level permits obtaining fundamental information regarding the relationship between structure and function/performance. The numerous advanced techniques offered by modern synchrotron sources give core means to provide structural windows into materials such as these. For more practical reasons, there is an increasing tendency and need to investigate these processes *in situ* in order to provide a true insight into how catalysts interact with the fuelled gas mixture under real working conditions on a variety of time scales. Such an *in situ* approach promises a more complete understanding of the functioning of these complex materials and thus the rational development of improved TWCs. The importance of the construction of suitable (from an X-ray probe and process point of view) *in situ* cells is therefore apparent. On the other hand, emulating the highly fluxional (feedstock composition/temperature) operating conditions of car catalysts, while collecting useful analyzable absorption data, poses a challenge to both scientists and engineers. Exhaust catalysts are transiently submitted to very high temperatures, and can momentarily reach up to 1300 K in modern cars. In addition, the exhaust gas composition itself fluctuates rapidly between oxidative and reductive atmospheres, the lambda cycle occurring on the order of a few seconds. These severe conditions influence the design of both the experiment and the catalytic cell itself. Conceptualizing them together as an inclusive entity is vital for obtaining significant and accurate results.

The aim of this paper is to present the design of two novel catalytic reactors optimized for an *in situ* X-ray absorption spectroscopy (XAS) investigation of commercial three-way catalysts working under realistic conditions.

The development of X-ray-compatible *in situ* cells for catalyst studies, either in a general sense or with more specific objectives, has a long history (see, for example, Kampers *et al.*, 1989; Couves *et al.*, 1991; Clausen *et al.*, 1991; Dent *et al.*, 1995; Meitzner *et al.*, 1998; Revel *et al.*, 1999; Ressler, 2003; Wienold *et al.*, 2003; Huwe & Fröba, 2004; Grunwaldt *et al.*, 2004; Bare *et al.*, 2006, 2007). Many techniques other than XAS, namely Fourier transform infrared spectroscopy and mass spectrometry, for example, have also been used in recent years to study, *in situ*, the evolution of these catalysts in order to reveal the relationship between their structure and reactivity, and to inspect the formation of intermediate species and products in a particular reactive environment (Rohe & Pitchon, 2001; Martínez-Arias *et al.*, 2001; Boaro *et al.*, 2004; Heeb *et al.*, 2004). However, the remarkable benefit of XAS studies lies in the ability to directly examine the oxidation state and local environment of the metallic catalytic centres, present as nanoparticles supported on an oxide support with high surface area, under temperatures and time scales close to those of real working conditions. Work in this field has been extensively carried out by Thomas & Sankar (2001), Topsoe (2003), Bare *et al.* (1999), Yi *et al.* (2003), Newton, Dent *et al.* (2007), Grunwaldt *et al.* (2006), Evans *et al.* (2007) and Beale *et al.* (2005), to mention just a few. Considering the complexity of these processes, a multi-technique approach that combines

‡ Current address: ALBA Synchrotron, Carretera BP 1413, Km 3.3, 08290 Cerdanyola del Vallès, Barcelona, Spain.

two or more of the techniques has increasingly been applied with great success providing unambiguous complementary information (Tinnemans *et al.*, 2006, and references therein).

In line with the stringent operational requirements of time resolution (in the milliseconds to few seconds range), the selection of X-ray absorption methodologies becomes highly restricted (Newton *et al.*, 2002), *i.e.* the piezo-QEXAFS and energy-dispersive XAS techniques. Both techniques have been shown to play a pivotal role in the elucidation of the reaction mechanisms of highly dynamic catalysts using the transmission mode (Lützenkirchen-Hecht *et al.*, 2005; Briois *et al.*, 2005; Newton, Belver-Coldeira *et al.*, 2007). However, in the case of commercial auto-exhaust catalysts, which contain a very low amount of precious metal dispersed on highly absorbing matrixes, *in situ* XAS experiments in transmission mode are very often not possible. Consequently, fluorescence acquisition is frequently the mode of choice for these types of experiments and adds the challenge of using suitable detection systems, and associated electronics/storage structures, that are able to fulfil subsecond time-resolution requirements.

The above-mentioned techniques, both well suited for studying catalytic reactions *in situ*, have their own advantages and restrictions. Piezo-QEXAFS is a recent optimization of the more standard quick-EXAFS method which has been used to measure fluorescence near-edge spectra of a very homogeneous sample (10 mmol l^{-1} solution of $CuSO_4$) in 55 ms with a reasonably good signal-to-noise (S/N) ratio (Lützenkirchen-Hecht *et al.*, 2001). This technology is currently being implemented on a number of synchrotron radiation XAS beamlines and the potential for research in this field is indubitably tremendous. The main limitation of the quick-EXAFS or piezo-QEXAFS method lies in the continuous movement (rotation) of the crystals and in the vertical oscillation of the beam exiting the monochromator.

The turbo-XAS approach developed by Pascarelli *et al.* (1999) on the energy-dispersive XAS beamline at the ESRF (ID24) takes advantage of some of the specificities of energy-dispersive XAS spectrometers, although acquisition is performed using sequential, not parallel, data acquisition. In particular, the stability of the energy scale and focal spot position remain unaltered during an energy scan, which is performed by scanning a slit on the polychromatic fan downstream of the polychromator. The main drawback in this scheme is related to the important flux reduction operated by the slit: the size of the slit opening is defined by a compromise between energy resolution and flux.

In the experiments described in this work, we have used the turbo-XAS approach in fluorescence mode. The limiting factor for time resolution is presently of the order of 100 ms for XANES, and is defined by the speed of the slit, the need to reverse the slit direction (bidirectional collection), and the readout electronics. Independently, it is worthwhile mentioning that other fields of research have also profited from the fluorescence turbo-XAS approach with a dispersive set-up (Pascarelli *et al.*, 2006; Muñoz *et al.*, 2006).

The aim of this paper is to describe the development of two new catalytic cells which have been conceptualized to fulfil the above-mentioned rigorous requirements for the *in situ* study of three-way catalysts. The specific characteristics of these catalytic cells together with the original experimental approach of choosing the turbo-XAS method using an energy-dispersive EXAFS beamline for real-time investigations have led to a new type of experiment and investigative possibilities.

2. *In situ* cells

The required features that the reported cells fulfil are the following: (i) collection of XAFS spectra in fluorescence mode; (ii) high temperatures achievable (1123 K and 1273 K on the sample for the two cell designs); (iii) ability to work under oxidizing/reducing atmospheres; (iv) gases can flow through the sample environment at high fluxes and they can be monitored in time with a mass spectrometer; (v) minimized dead volume; (vi) contain sample holder for pellets of diameter 5 mm (this can be adapted for other pellet sizes); (vii) small cell, easy to handle.

These cells can only hold samples in pressed pellet form. This final design was restricted by the aforementioned industrial users' needs and priorities. The sample presentation and the cell design have to be borne in mind in order to plan a proper and meaningful experiment, thus reaching the best compromise between spectroscopy and catalysis. It is known that limitations due to film and pore diffusion may occur owing to flow conditions, catalyst shape, reactor design and material, if any, that serves to dilute the catalyst. For instance, the reduction kinetics of CuO/ZnO in 5% H_2/He is different for a plug-flow system (the reaction is considerably faster) than for a pellet cell, and this difference has been attributed either to mass transfer limitations or different flow conditions in the cells (Grunwaldt *et al.*, 2004). Although a plug-flow system is generally preferred because it represents more realistic catalytic conditions and the resistance for pore diffusion is minimal, cells containing pellets can also give similar results in those cases where temperature ramp rates and flow conditions are adequately controlled and pore diffusion of the molecules is sufficiently fast. Therefore, cells with pressed pellets are not always a barrier to obtaining meaningful results; it will depend on the piece of information one is looking at and how the results are interpreted. In addition, a pressed pellet has the advantage over a powdered sample that it is more homogeneous, leading to a better S/N ratio, and temperature measurements can generally be obtained more accurately.

For convenience we have given the two *in situ* cells the names 'Thermocoax cell' (the company of the heating element) and 'Maxthal cell' (the material of the heating element). The Thermocoax cell has been optimized to perform catalytic reactions under strictly trace-element-free conditions whereas the Maxthal cell has been optimized for high-temperature studies.

2.1. Thermocoax cell

This reactor cell is formed by three main parts: (i) the heating chamber, (ii) the reactive chamber, which lodges (iii) the sample holder. This compact cell has cylindrical symmetry, compatible with the required very small volume of the reactive chamber, and covers a range of temperatures between 298 and 1123 K measured on the sample, bringing about a uniform temperature distribution on the sample.

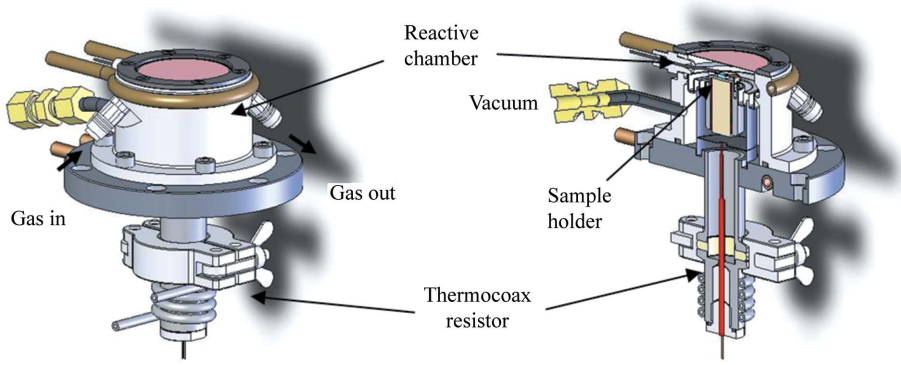

Figure 1
Full view and sectioned view of the design of the Thermocoax cell.

A schematic view of the furnace is presented in Fig. 1. The heating element is a sheathed coaxial resistor of diameter 1 mm. The resistor is spring-shaped. The heater is adjusted inside the sample holder; this improves the thermal transfer to the sample and reduces the inertia. The maximum accepted electrical power is about 150 W. The temperature of the heater is controlled by a Eurotherm, and the maximum rate of heating or cooling is limited to 300 K h^{-1} to avoid the thermal shock of the heating element. Under these conditions the heater life time is about three to eight days at 1123 K.

A stainless steel membrane welded on the cylindrical flange of the heating chamber forms the separation between the heating chamber and the reactive chamber. This is of paramount importance in catalysis when working at such high temperatures so as to avoid trace contamination of the sample, which can tremendously impinge on the system reactivity. Furthermore, the shape and thickness (optimal thickness of 200 µm) of the membrane has been designed with the aim of minimizing thermal losses whilst ensuring a good thermal exchange with the sample. Fig. 2 depicts the membrane.

The tailored inconel clip that holds the sample is fixed on top of the central part of the stainless steel dividing membrane (see Fig. 2). This clip has been designed to maintain good thermal contact with the sample and to accommodate pellet samples with an effective diameter of a few millimeters and thickness between 0.5 and 1 mm. This arrangement though can be readily adapted for pellet samples of other dimensions.

The heating chamber of the cell is designed to work under vacuum (about 10^{-6} mbar) in order to avoid heat dispersion and therefore decrease the effective sample temperature. A circular reflective stainless steel screen of thickness 0.1 mm is placed around the inconel holder of the reactor to reduce thermal losses.

On the sides of the reactive chamber, opposite to each other, are the gas inlet and gas outlet, with push-on fittings and adaptable to 1/16 inch stainless steel gas capillaries. This configuration allows high gas-flow rates. The reactive chamber has dimensions of 40 mm diameter and 9.5 mm height. A machined Macor piece is integrated inside the chamber to reduce the dead volume to 7.4 cm^3. A small dead volume is important in heterogeneous catalysis to obtain fast gas response. This ceramic insert also serves to reduce heat dissipation. The chamber is hermetically closed with a circular

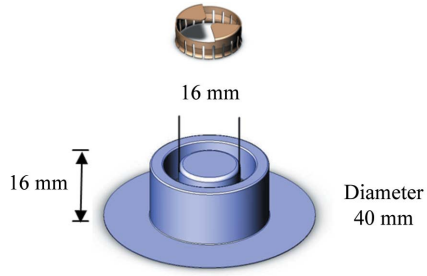

Figure 2
Dividing stainless steel membrane that separates the heating chamber from the reacting chamber. An inconel clip is placed on the top to hold the sample.

Kapton window (thickness 25 µm and diameter 30 mm) held by a customized stainless steel washer. The separation of the Kapton window from the heating source is 5.5 mm, the Kapton achieving a maximum temperature of 400 K when the sample is at 1123 K owing to the efficient cooling system.

The external part of the cell, which wraps around the reactive chamber, is composed of a stainless steel cylinder cooled by water running at high flow to avoid burning the Kapton window and prevent overheating of the fluorescence detector (Si-diode), the latter placed at only 9 mm from the top of the sample.

To control the temperature, a K chromel–alumel thermocouple is set into a carefully polished stainless steel disc placed below the sample in order to obtain a realistic reading of the sample temperature. At 1123 K, thermal stability can be attained after 5 min with a maximum gradient of 5 K. This efficient control of isothermals applies to the entire heating process. Whilst the temperature below the sample is read by the K thermocouple connected to a Eurotherm device, the sample temperature can equally be read *in situ* by a pyrometer (over 675 K) through the Kapton window.

2.2. Maxthal cell

A new reactor cell has been built for the study of TWCs, similar to the previous cell but optimized to perform high-temperature studies. The main additional feature of this cell is that it can reach temperatures up to 1273 K on the sample with

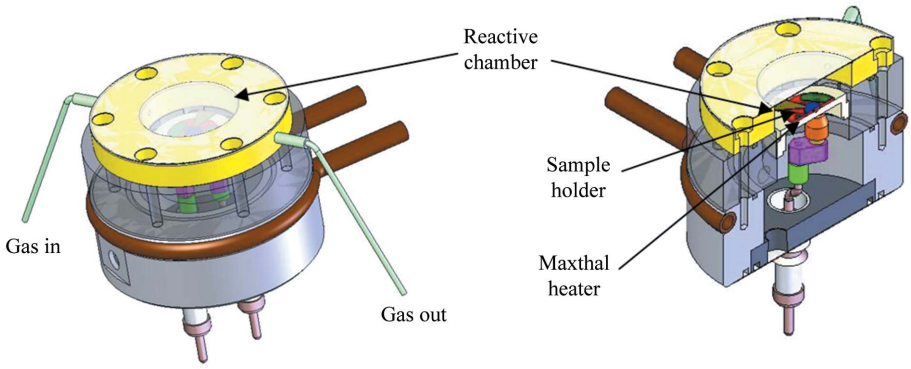

Figure 3
Full view and sectioned view of the design of the Maxthal cell.

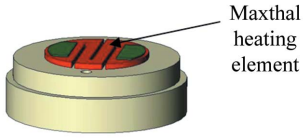

Figure 4
View of the circular Maxthal heating element cut in a zigzag configuration and supported on a BN block.

the aim of studying possible redispersion behaviour of the Pt-based catalysts.

Such high temperatures are achieved using a Maxthal heating element. Maxthal material possesses a combination of properties essential for high-temperature non-stick coating applications. This material is remarkably resistant to thermal shock, wear, oxidation and corrosion; it is tough and a good electrical and thermal conductor.

Fig. 3 illustrates the reactor cell. A Maxthal 211 (Ti_2AlC) heating element is machined into a circular form (diameter 15 mm, thickness 0.5 mm). The disc is cut in a zigzag shape to increase its resistivity (see Fig. 4). This heating element is mounted on a flexible mechanical adaptation to avoid stress and pressure on the Maxthal heater while heating up to high temperatures. The isolating interface between the heater disc and the electrical holder part is made of boron nitride.

The original in-house idea of welding two stainless steel electrical connectors onto the heater disc permits the passage of strong currents through the system, avoids undesired oxidation of the cell elements and keeps the system undisturbed for the entire experiment. The maximum accepted electrical power is about 220 W. The maximum heating or cooling rate is limited to 600 K h^{-1} by the Maxthal expansion. This rate is twice as fast as in the previous cell. In this case, however, longer times are needed to obtain a uniform temperature distribution on the sample. The heater lifetime is about 16 h at 1273 K on the sample and three days at 1173 K.

The overall outline of the cell is very similar to that of the Thermocoax cell. The electrical part of the cell, however, does not need to be kept in a vacuum. The dimensions of the water-cooled circular reactive chamber are 28 mm diameter and 8 mm height. This leaves a dead volume of only 4.5 cm^3. This chamber is hermetically closed with a Kapton window held with a stainless steal washer. During the experiment a compressed-air gun is used to avoid damaging the Kapton window.

The pellet sample (5 mm × 0.5 mm) is placed directly onto the Maxthal heater, although a thin interface layer of boron nitride coating is used to avoid sample stickiness. The sample is held using a tailored inconel clamp. Temperature regulation is managed by a Eurotherm device. A K chromel–alumel thermocouple, placed on top of the sample and below the inconel clamp, reads the temperature of the sample. At the same time, for further verification, the sample temperature can also be measured *in situ* using a pyrometer, calibrated previously.

3. Experimental

The Thermocoax and Maxthal cells have been tested on the undulator dispersive-EXAFS beamline ID24 of the ESRF operating at 200 mA of stored current. The XANES measurements were carried out at the Pt L_3-edge (11565 eV) on several Pt samples potentially used as TWCs at 1 kHz sampling rate. The polychromator was equipped with a Si(111) crystal; the turbo-XAS acquisition mode was used. The moving transversal slit placed upstream of the polychromator was opened to 120 µm; this opening did not affect the overall energy resolution of the beamline. This methodology permitted continuous acquisition of fluorescence spectra of low-loaded Pt samples containing highly absorbing matrixes, otherwise impossible to measure in transmission, while taking advantage of the quick data collection reaching the subsecond to second range. This time resolution is compatible with the lambda cycle at which catalytic exhaust converters are submitted during driving. The measurements performed with both Thermocoax and Maxthal cells were found to be of the same spectroscopic quality.

Fig. 5 exemplifies the difficulties involved in measuring energy-dispersive XANES spectra in transmission mode for a TWC containing 2 wt% Pt dispersed on a highly absorbing support made of pure cerium–zirconium–yttrium mixed oxide (CZY) (Nagai *et al.*, 2008). The acquisition time for the fluorescence spectra is 1.1 s. In this case and for this particular sample the S/N ratio is 1.5 × 10^3. This is an acceptable value for investigating *in situ* the dynamics of these catalysts. This S/N ratio was calculated as the effective number of counts considering the signal as the difference between the number of photons above the edge and the number of photons below the edge, and the noise as the square root of the number of photons above the edge.

For the *in situ* XAS measurements, pellets of different Pt loadings dispersed on highly absorbing supports were pressed so as to obtain discs of diameter 5 mm and thickness 0.5 mm. The catalysts were not mixed with the low-porosity and low-surface-area BN compound in order to avoid pore diffusion limitations as well as changes in the thermal properties of the

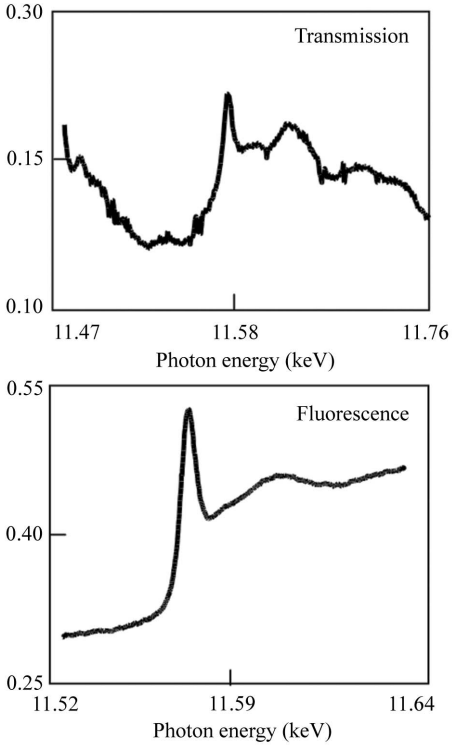

Figure 5
Comparison of the XANES region of spectra taken on the dispersive beamline ID24 (ESRF) at the Pt L_3-edge. The sample contains 2 wt% Pt dispersed on a mixed oxide support containing pure ceria–zirconia–ytria (Nagai *et al.*, 2008). Top: taken in transmission (acquisition time 3.8 s). Bottom: taken in fluorescence using turbo-XAS (acquisition time 1.1 s).

system. The pellets were placed inside the reactor cell. Two Si-diode detectors were used to collect both the incident (I0) and the fluorescent (I1) radiation. The flexibility of the *in situ* cells allows positioning of the two Si-diode detectors very close to the sample. The I0 diode is placed perpendicularly with respect to the beam and collects the elastically scattered X-rays from a Kapton foil of thickness 130 µm. The I1 diode is placed facing the sample and is oriented perpendicular to the incident beam direction in order to minimize elastically scattered radiation. The I1 diode is placed very close to the sample (9 mm apart) to maximize the solid angle available for photon collection. Owing to its proximity to the heating element, the I1 diode is water-cooled down to 283 K. The signals from the diodes are converted and amplified by two Stanford SR 570 current-to-voltage preamplifiers. Furthermore, a gas flow system regulated by mass flow controllers permits the control of the oxidative and reducing atmospheres that are introduced in the cell. A remotely controlled switching valve allows swapping between gas conditions. This valve is placed very close to the sample environment in order to minimize the dead volume (down to 6×10^{-2} cm^3 before reaching the cell). The set-up of the valve is configured to minimize back-pressure problems. Additionally, a quadrupole mass spectrometer monitors continuously and in time the reactivity of the main gas components. Fig. 6 shows a photograph of the set-up. The scheme of this set-up can be viewed in the publication of Nagai *et al.* (2006).

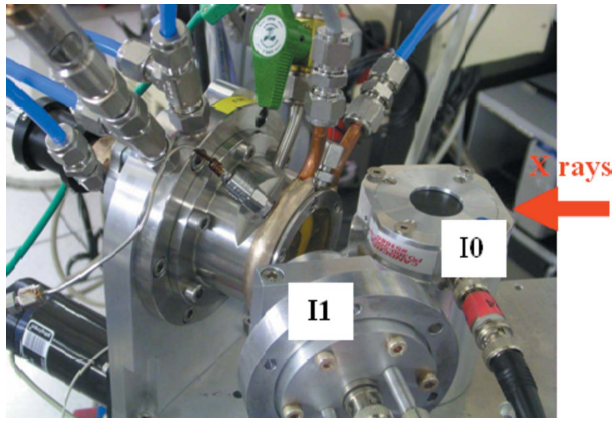

Figure 6
Photograph showing the arrangement of the *in situ* XAS cell and the measuring diodes (I0 and I1) on the beamline.

Very promising results have been obtained as a result of studies of Pt catalysts performed by Toyota with this set-up. The analysis of these results is out of the scope of this paper; a thorough interpretation of some of these results can be found elsewhere (Nagai *et al.*, 2006, 2008, 2009). Nonetheless, in this paper we will provide a general description of the type of experiments carried out by Toyota in the dynamic study of TWCs under realistic conditions; we will also illustrate the type of data obtained using the Thermocoax and Maxthal cells in a turbo-XAS set-up in extreme cases.

In a typical experiment, different loadings (2 wt%, 1 wt% and 0.5 wt%) of Pt dispersed on a variety of highly absorbing matrixes have been synthesized in order to dynamically investigate the sintering/redispersion phenomena of real exhaust catalysts, in real time and under realistic reaction conditions. To do this, temperature-programmed experiments at different stages (ramps of 7 K min^{-1}) were carried out, starting from room temperature up to typically 1123 K (1273 K for the case of the Maxthal cell). During these experiments, oxidizing (4 or 20% O_2/He) and reducing (3% H_2/He) atmospheres were switched every 30 s. Pt L_3-edge XANES fluorescence spectra were collected continuously with an integration time in the range of seconds (which appeared to be sufficient to follow dynamically the sintering/redispersion process, though in some instances a subsecond resolution was used), and during the time that the entire temperature-programmed cycled experiment took place (typically 11 h). In these long but quick experiments, the long-term stability, successfully attained by the dispersive optics and sample environment, is obviously critical.

Fig. 7 shows XANES spectra taken in fluorescence of 1 and 0.5 wt% Pt samples dispersed on a CZY support containing traces of other heavy elements. These were taken *in situ* at 673 K and under oxidizing and reducing atmospheres. The spectra were measured in 6 s for the 1 wt% Pt samples and in 5.8 s for the 0.5 wt% Pt samples, which seems to be sufficient for the given experiment. The S/N ratios of these spectra are 0.8×10^3 for the 1 wt% Pt samples and only 0.2×10^3 for the 0.5 wt% Pt samples, these S/N ratios being calculated as previously mentioned. It can be seen though that on the

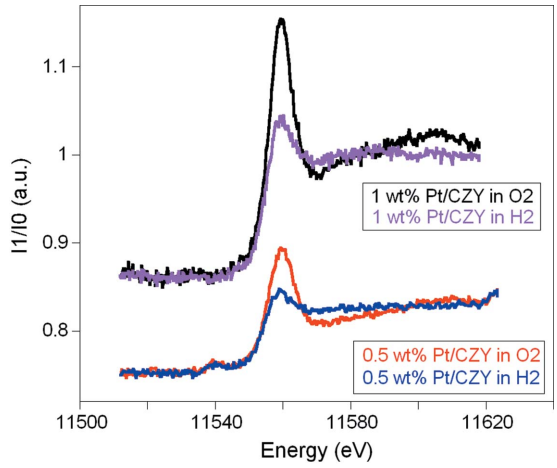

Figure 7
Pt L_3-edge fluorescence XANES spectra of 1 wt% (top) and 0.5 wt% (bottom) Pt samples dispersed on CZY with traces of other heavy elements, submitted to oxidizing (20% O_2/He) and reducing (3% H_2/He) atmospheres at 67 K. Spectra of 1 wt% Pt samples are measured in 6 s, and those of 0.5 wt% Pt samples in 5.8 s.

0.5 wt% Pt spectra a glitch at 11540 eV begins to be perceptible.

This type of low-Pt-content sample, highly inhomogeneous and extremely absorbing, could be measured, although with some difficulty, down to 900 ms over the XANES region, as shown in Fig. 8. The usefulness of the data, in terms of quality, depends greatly on the type of information needed. In our case, the quality was sufficient for measuring, after normalization, the height of the white line to study quantitatively the redispersion process up to 1173 K. Clearly, if the experiments permit, S/N ratios can be improved by averaging several spectra or by simply collecting the spectra for longer times. Moreover, Fig. 8 exhibits the high reproducibility of the system given that each of these spectra is made of five consequently recorded spectra with almost no dead time between scans.

Fig. 9 exemplifies the improvement of the data quality when the CZY matrix of the 0.5 wt% Pt sample is replaced by a less absolving matrix as is the case of 10% ceria–zirconia on alumina. The XANES spectrum, which was measured at a time resolution of 830 ms, manifests the much lower background contribution and therefore enhances the quality of the data by over a factor 20, the S/N ratio in this case being 13×10^3.

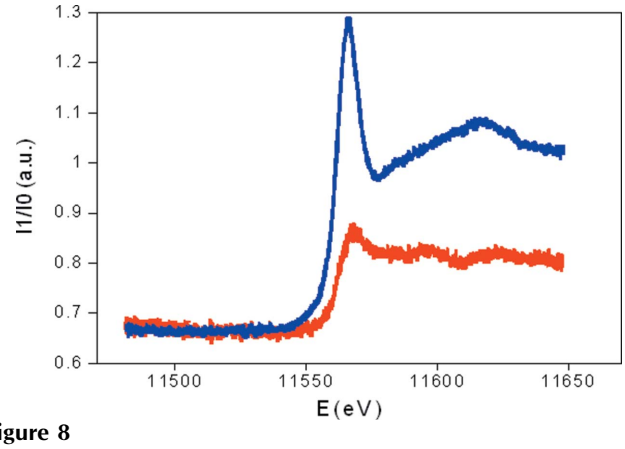

Figure 8
Pt L_3-edge XANES spectra measured at room temperature in fluorescence turbo-XAS mode of a 2 wt% Pt/CZY sample (reduced form, top) and 0.5 wt% Pt/CZY sample (oxidized form, bottom). Each of these spectra comprises five subsequent spectra of 900 ms each.

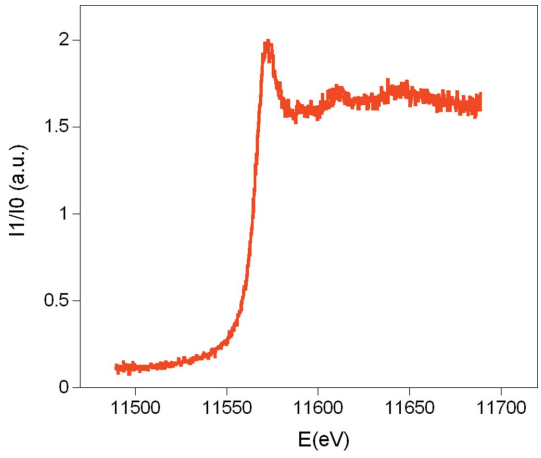

Figure 9
Pt L_3-edge XANES spectrum measured at room temperature in fluorescence turbo-XAS mode of 0.5 wt% Pt dispersed on 10% ceria–zirconia on alumina. The XANES spectrum shown comprises two spectra measured at 830 ms each.

4. Conclusions

Two new XAFS *in situ* cells have been conceived to work in fluorescence mode. Although these cells have been aimed at studying commercial TWCs under tight design constraints, their flexibility and very small size make these instruments particularly handy and versatile for other techniques and experiments. A major feature of these cells is the elevated temperatures attained (up to 1123 K and 1273 K) while resisting to oxidative and reducing atmospheres. This is possible owing to the strict isolation of the reactive chamber from the heating element, as in the case of the Thermocoax cell, and the high resistance to oxidation properties of the Maxthal material. Additionally, the minimization of the overall cell design provides the possibility of placing the detector very close to the sample, thus allowing collection of better signal without damaging any of the set-up elements. Notwithstanding, there are also some limitations associated with these cells: they can only hold pellet samples; the Thermocoax cell is limited in temperature to 1123 K, which is sometimes exceeded in modern cars; and in the Maxthal cell the temperature ramp needs to be more accurately controlled to obtain a uniform distribution of temperature across the sample. These cells have been used for the first time on the dispersive-EXAFS beamline of the ESRF, ID24, using the turbo-XAS technique for the *in situ* study of three-way catalysts under realistic conditions that mimic an exhaust of a car. Some illustrative examples have been presented to demonstrate the potential of the complete set-up and experiment. Nonetheless, it is foreseen that these cells will soon find

applications in a fan of scientific areas opening new appealing experimental possibilities in material science.

We would like to thank Florian Perrin, Sebastien Pasternak and Marie-Christine Dominguez for their technical support. We also acknowledge Yasuo Ikeda and Nobuyuki Takagi of Toyota for their contributions.

References

Bare, S. R., Mickelson, G. E., Modica, F. S., Ringwelski, A. Z. & Yang, N. (2006). *Rev. Sci. Instrum.* **77**, 023105.
Bare, S. R., Modica, F. S. & Ringwelski, A. Z. (1999). *J. Synchrotron Rad.* **6**, 436–438.
Bare, S. R., Yang, N., Kelly, S. D., Mickelson, G. E. & Modica, F. S. (2007). *AIP Conf. Proc.* **882**, 622–624.
Beale, A. M., van der Eerden, A. M. J., Kervinen, K., Newton, M. A. & Weckhuysen, B. M. (2005). *Chem. Commun.* **24**, 3015–3017.
Boaro, M., Giordano, F., Recchia, S., Dal Santo, V., Giona, M. & Trovarelli, A. (2004). *Appl. Catal. B*, **52**, 225–237.
Briois, V., Lützenkirchen-Hecht, D., Villain, F., Fonda, E., Belin, S., Griesebock, B. & Frahm, R. (2005). *J. Phys. Chem. A*, **109**, 320–329.
Clausen, B. S., Steffensen, G., Fabius, B., Villadsen, J., Feidenhansl, R. & Topsoe, H. (1991). *J. Catal.* **132**, 524–535.
Couves, J. W., Thomas, J. M., Waller, D., Jones, R. H., Dent, A. J., Derbyshire, G. E. & Greaves, G. N. (1991). *Nature (London)*, **354**, 565–577.
Dent, A. J., Greaves, G. N., Roberts, M. A., Sankar, G., Wright, P. A., Jones, R. H., Sheehy, M., Madill, D., Catlow, C. R. A., Thomas, J. M. & Rayment, T. (1995). *Nucl. Instrum. Methods Phys. Res. B*, **97**, 20–22.
Evans, J., Puig-Molina, A. & Tromp, M. (2007). *MRS Bull.* **32**, 1038–1043.
Grunwaldt, J.-D., Caravati, M. & Baiker, A. (2006). *J. Phys. Chem. B*, **110**, 9916–9922.
Grunwaldt, J.-D., Caravati, M., Habnnemann, S. & Baiker, A. (2004). *Phys. Chem. Chem. Phys.* **6**, 3037–3047.
Heeb, N. V., Forss, A. M., Saxer, C. J., Wilhelm, P., Bruhlmann, S., Rudy, C. & Weilenmann, M. F. (2004). *Int. J. Environ. Pollut.* **22**, 287–300.
Huwe, H. & Fröba, M. (2004). *J. Synchrotron Rad.* **11**, 363–365.
Kampers, F. W. H., Maas, T. M. J., van Grondelle, J., Brinkgreve, P. & Koningsberger, D. C. (1989). *Rev. Sci. Instrum.* **60**, 2636–2638.
Lützenkirchen-Hecht, D., Grundmann, S. & Frahm, R. (2001). *J. Synchrotron Rad.* **8**, 6–9.
Lützenkirchen-Hecht, D., Grunwaldt, J.-D., Richwin, M., Griesebock, B., Baiker, A. & Frahm, R. (2005). *Phys. Scr.* T**115**, 831–833.
Martínez-Arias, A., Fernández-García, M., Hungría, A. B., Conesa, J. C. & Soria, J. (2001). *J. Alloys Comput.* **323**, 605–609.
Meitzner, G., Bare, S. R., Parker, D., Woo, H. & Fischer, D. A. (1998). *Rev. Sci. Instrum.* **69**, 2618–2621.
Muñoz, M., De Andrade, V., Vidal, O., Lewin, E., Pascarelli, S. & Susini, J. (2006). *Geochem. Geophys. Geosyst.* **25**, Q11020.
Nagai, Y., Dohmae, K., Ikeda, Y., Takagi, N., Tanabe, T., Hara, N., Guilera, G., Pascarelli, S., Newton, M. A., Kuno, O., Jiang, H., Shinjoh, H. & Matsumoto, S. (2008). *Angew. Chem. Int. Ed.* **47**, 9303–9306.
Nagai, Y., Dohmae, K., Teramura, K., Tanaka, T., Guilera, G., Kato, K., Nomura, M., Shinjoh, H. & Matsumoto, S. (2009). *Catal. Today*. In the press.
Nagai, Y., Takagi, N., Ikeda, Y., Dohmae, K., Tanabe, T., Guilera, G., Pascarelli, S., Newton, M., Shinjoh, H. & Matsumoto, S. (2006). *AIP Conf. Proc.* **882**, 594–596.
Newton, M. A., Belver-Coldeira, C., Martínez-Arias, A. & Fernández-García, M. (2007). *Nat. Mater.* **6**, 528–532.
Newton, M. A., Dent, A. J. & Evans, J. (2002). *Chem. Soc. Rev.* **31**, 83–95.
Newton, M. A., Dent, A. J., Fiddy, S. G., Jyoti, B. & Evans, J. (2007). *Catal. Today*, **126**, 64–72.
Pascarelli, S., Mathon, O., Muñoz, M., Mairs, T. & Susini, J. (2006). *J. Synchrotron Rad.* **13**, 351–358.
Pascarelli, S., Neisius, T. & De Panfilis, S. (1999). *J. Synchrotron Rad.* **6**, 1044–1050.
Ressler, T. (2003). *Anal. Bioanal. Chem.* **376**, 584–593.
Revel, R., Bazin, D., Seigneurin, A., Barthe, P., Dubuisson, J. M., Decamps, T., Sonneville, H., Poher, J. J., Maire, F. & Lefrancois, P. (1999). *Nucl. Instrum. Methods Phys. Res. B*, **155**, 183–188.
Rohe, R. & Pitchon, V. (2001). *Top. Catal.* **16**, 311–315.
Thomas, J. M. & Sankar, G. (2001). *J. Synchrotron Rad.* **8**, 55–60.
Tinnemans, S. J., Mesu, J. G., Kervinen, K., Visser, T., Nijhuis, T. A., Beale, A. M., Keller, D. E., van der Eerden, A. M. J. & Weckhuysen, B. M. (2006). *Catal. Today*, **113**, 3–15.
Topsoe, H. (2003). *J. Catal.* **216**, 155–164.
Wienold, J., Timpe, O. & Ressler, T. (2003). *Chem. Eur. J.* **9**, 6007–6017.
Yi, W., Schwidder, M. & Grünert, W. (2003). *Catal. Lett.* **86**, 113–119.